Stall Margin Enhancement of Aeroengine Compressor with a Novel Type of Alternately Swept Blades

Chao Fang

Master Candidate, School of Aeronautics and Astronautics,

Shanghai Jiao Tong University,

Shanghai, China

E-mail: fcchao0416@126.com

Yizhi Zhang

Master Candidate, School of Aeronautics and Astronautics,

Shanghai Jiao Tong University,

Shanghai, China

E-mail: Itszyz919@sina.com

Yidan Li

Master Candidate, School of Aeronautics and Astronautics,

Shanghai Jiao Tong University,

Shanghai, China

E-mail: yidanli@sjtu.edu.cn

Xiaohua Liu[1]

Assiatant Professor, School of Aeronautics and Astronautics,

Shanghai Jiao Tong University,

Shanghai, China

E-mail: Xiaohua-Liu@sjtu.edu.cn

Abstract: Rotating stall, as a typical kind of flow instability in aero-compressor, could lead to disastrous consequences of aeroengine. Therefore, an effective method is perused to enhance the stall margin. Some of the previous researches focus on the holistically swept rotor. This paper concentrates on the impact of a novel type of axial swept blades on the aerodynamic behavior of transonic axial-flow compressor rotors. A CFD package, which solves the Reynolds-averaged Navier-Stokes equations, is used to compute the complex flow field of the compressor. It is validated against the existing experimental data. Comparisons with experimental data indicates that the overall features of the rotor performance are calculated well by the numerical solution with acceptable accuracy. A number of new swept rotors were modelled based on the original blade, by axially moving

[1] Corresponding author

the location of blade alternately. All the new rotors are simulated and comparison of the results shows that the alternately swept rotor enhances the stall margin effectively. The stall margin of new rotors can reach up to 18.16%, while that of the original rotor is only 9.71%. More physical explanations on the stall margin improvement are given based on a detailed analysis of the flow field.

Keywords: aeroengine compressor, stall margin, alternate swept blade, numerical simulation

1 Introduction

With the increase of compressor stage load, the secondary-flow in the blade passages are more three-dimensional, the tip leakage is more serious, and the boundary layer and corner region are more easily separated[1]. Therefore, the requirement for stable operating margin of compressor is more stringent. There is a certain contradiction between pursuing higher stage pressure ratio and improving the stall margin of compressor. In order to enhance the stall margin of the compressor, the methods can be adopted by the compressor at present include variable guide vanes[2, 3], casing treatment[4], air bleeding[5], birotor and trispool. Most of these methods have been applied in engineering and achieved good results.

Vo et al.[6] used a computational study to define the phenomena that lead to the onset of short length-scale (spike) rotating stall disturbances and got two conditions for the formation of spike disturbances[7, 8], both of which are linked to the tip clearance flow. One is that the interface between the tip clearance and oncoming flows becomes parallel to the leading-edge, which would lead to the spike. The second is the initiation of backflow, stemming from the fluid in adjacent passages, at the trailing-edge plane.

The effects of swept rotor on the overall aerodynamic performance and compressor stability have been widely analysed in the open literature[9-11]. Hah et al.[12] conducted numerical and experimental analysis on an unswept rotor, a forward-swept rotor, and a backward-swept rotor by solving Reynolds-averaged Navier-Stokes equations. He pointed out that the forward-swept rotor brings a larger stall margin than the unswept rotor, and that the backward-swept rotor has the opposite effect on overall performance. Wadia et al.[13] obtained similar results and provieded a physical description about reducing shock/boundary layer resulting from a locally low loading at the tip of forward-swept rotor. Dentao and Xu[14] observed the overall aerodynamic performance of swept rotor and the results of backward-swept rotor and forward-swept rotor showed that the efficiency is not very remarkable. The common conclusion was obtained by Chen He et al.[15] in four kinds of swept rotors simulation including forward axial swept, forward chordwise swept, backward axial swept, and backward chordwise swept which are modified the position of tip blade section.

According to the research of Vo et al.[6], tip clearance flow will affect adjacent blade passages. The present paper concentrates on the impact of a novel type of alternately swept blades. We first introduce the design specification of test rotor and the novel types were defined here. Secondly, the comparison of the numerical and experimental results of the original rotor would show the accuracy of the steady CFD model. After that, all the new swept rotors were simulated to investigate the effects of alternately swept on the overall performance and stall margin. Finally, the comparison of all simulation was presented and the flow field would be analysed.

2 Rotor Geometries Definition

2.1 Original Rotor Type

A transonic axial compressor rotor, NASA Rotor 37 was used as original rotor type in this paper. The rotor 37 was designed by NASA Lewis Research Center. The design specification of this rotor is showed in Table 1. The rotor has 36 blades with the tip clearance of 0.335mm. The operating rotating speed was 17188 rpm, while pressure ratio and mass flow rate were 2.106 and 20.19 kg/s at operating point. The overall aerodynamic performance and detail flow field was provided by Reid and Moore[16]. Figure 1 Measurement stations shows the measurement stations in this paper. Our flow results were undertaken for station 1 and 4.[17]

Table 1 Design specification of Rotor 37[18]

Parameter	Value
Blade number	36
Total pressure ratio	2.106
Hub-tip ratio	0.7
Aspect ratio	1.19
Tip solidity	1.29
Tip clearance	0.0335 mm
Massflow	20.19 kg/s
Rotating speed	17188 rpm
Tip speed	454 m/s
Adiabatic efficency	0.877

2.2 Swept Rotors

We adopt rotor 37 as the original rotor and obtained some new rotors by axially moving the location of blade

alternately. The definition of sweep is showed in Figure 2 The definition of sweep Three types of rotors were modelled based on rotor 37. Type 1 refers to the original rotor. Type 2 refers to the rotor forward axially moving the location of blades holistically for 0.001m. Type 3 refers to the rotor which is obtained by forward axially moving the location of blades alternately for 0.001m. Type 4 refers to the rotor which is obtained by forward axially moving the location of blades alternately for 0.002m.

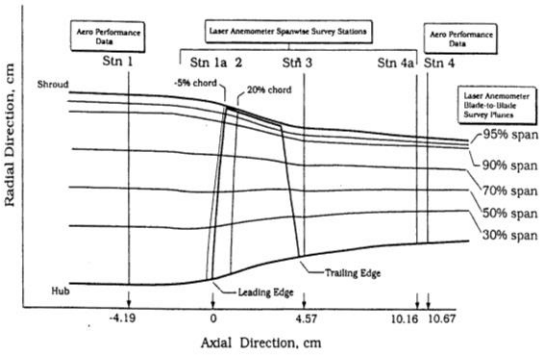

Figure 1 Measurement stations[19]

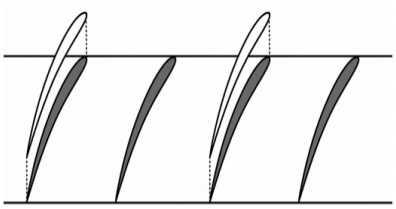

Figure 2 The definition of sweep

3 Model Validation

3.1 Computational Grid

The multi-block structured grid, of about 1300000 cells, was showed in Figure 3. Two passages were generated in one computational domain. An H-type grid was used for the main flow region, while a composite H/O type grid was generated in tip clearance region. The whole grid consisted of 146 cells in azimuthal direction, and 49 cells in spanwise direction, and 177 cells in streamwise direction. The cell width on solid walls was less than 1×10^{-6}.

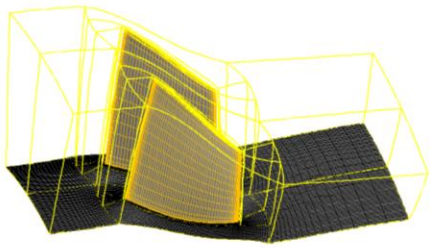

Figure 3 The computional grid for two passages

3.2 Comparison Between the Experiment and Calculation

For all the investigated rotor geometries, the flow field was computed in same conditions. The rotating speed was fixed to 17188 rpm for all rotor types, the inlet total pressure and total temperature were set to $p_{01}=101325Pa$ and $T_{01}=288.15K$. The convergence criteria were fixed to 1×10^{-6}. Steady state solutions were computed using S-A turbulence model[20]. The experimental data was investigated from AGARD test case report[19].

The experimental data and calculation results are presented in Figure 4. The measured and calculated mass flow rate were normalized using the corresponding mass flow at choke point. Our model predicted well the choking point, which was computed a value of 20.915 kg/s against the experiment one of 20.93 kg/s. The adiabatic efficiency is fell by slightly less (about 3.6%) than experiment in peak zone, while the calculated total pressure ratio achieved a great agreement with the experimental data. Figure 5 shows the spanwise distributions of pitch-averaged total pressure ratio, total temperature ratio and adiabatic efficiency at station 4 for choke point. The calculated profiles get an acceptable result with the experimental data.

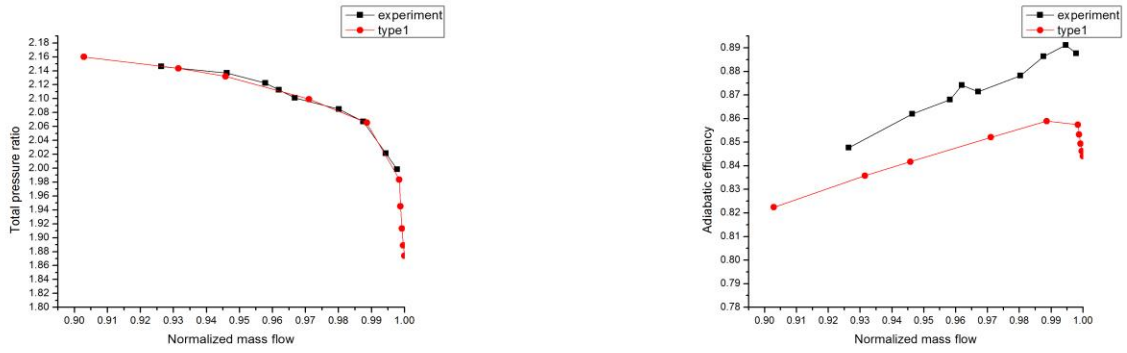

Figure 4 The performance maps for experiment and calculation of original type

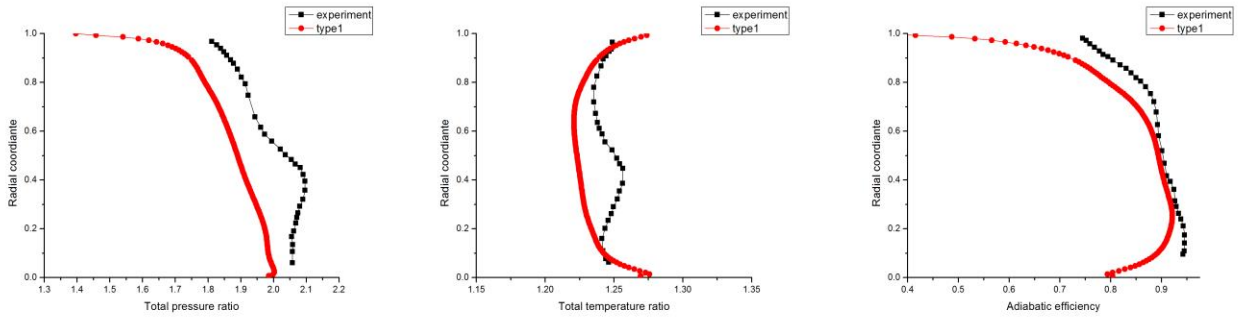

Figure 5 The radial results at station 4 for choke point

4 Simulation Results and Analysis

4.1 Overall Features

All the novel types were simulated by solving the Reynolds-averaged Navier-Stokes equation with S-A turbulence model. For these alternate and unaltered rotors, we adopt the same computational setting including the boundary conditions and grid setting as we showed previously.

The performance comparisons with all novel rotor types are presented in Figure 6. From Figure 6, the performance of type 2 is similar with type 1 for a slightly difference in low mass flow region. The rotor swept holistically means a small influence in the overall features of rotor. But, the two types (type 3 and type 4) with rotor swept alternately show an obvious change with the original rotor type. The efficiency of type 3 and type 4 is slightly underestimated in the peak zone (by about 0.93% and 1.16%), while the total pressure ratio is slightly underestimated by about 1.53% and 2.82%. The stall margin enhancement is showed in Table 2. The stall margin was calculated by

$$SM' = \frac{q_{md} - q_{ms}}{q_{md}} \times 100\% \quad (1)$$

where q_{md} is the mass flow rate of choke point and q_{ms} is the mass flow rate of near-stall point.

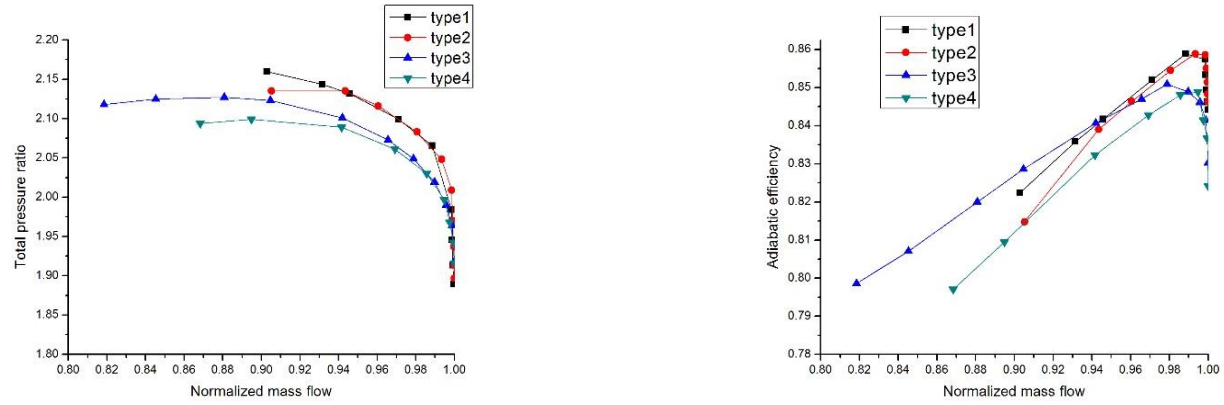

Figure 6 Performance maps of all rotor types

Table 2 The stall margin for all types

	q_{md} (kg/s)	q_{ms} (kg/s)	Stall margin
Type 1	20.915	18.884	9.71%
Type 2	21.04	19.045	9.48%
Type 3	20.93	17.13	18.16%
Type 4	20.982	18.22	13.16%

The stall margin of type 3 can reach up to 18.16%, while that of the original rotor type 1 is only 9.71%. Moreover, type 4 achieved a slightly higher stall margin by 13.16%. The novel types of rotor swept alternately obtained a great achievement in stall margin improvement.

Figure 7 compares the spanwise distribution of the total pressure ratio, total temperature ratio and adiabatic efficiency of all rotor types at choking mass flow. Clearly, for all three performance quantities, type1 are similar with these of type 2. The previous viewpoint about the influence of rotor swept holistically is approved by the spanwise distribution files. Between 30% and 70% span height, for both two alternate swept rotors, a slightly negative performance of adiabatic efficiency can be observed. On the other hand, these two rotor types obtain a positive performance of total pressure ratio and temperature ratio in same span height. This is a direct consequence of the tip clearance induced by the blade swept alternately, which will be analyzed below.

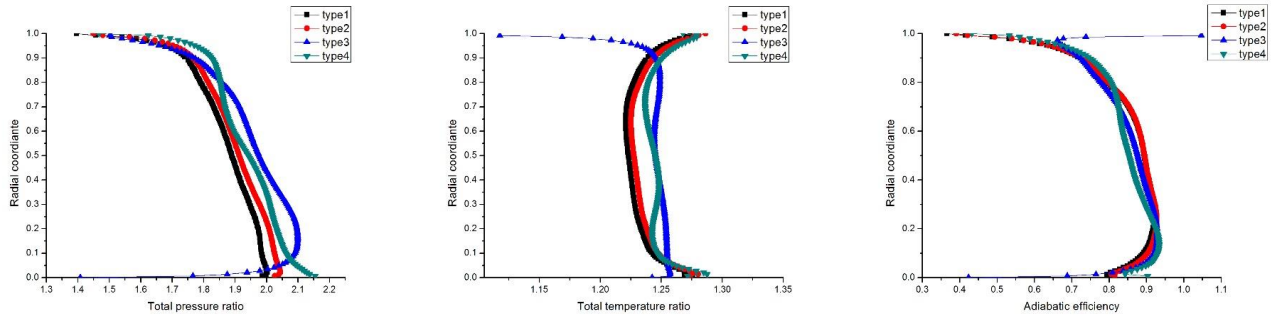

Figure 7 The radial results of four types at choke point

4.2 Tip Clearance Flow Fields Analysis

Figure 8 shows the relative Mach number contour at 95% span. It is also the comparison for 4 rotor types at three different mass flow points (100% choking mass flow, 96% choking mass flow, near-stall point). For all rotor types,

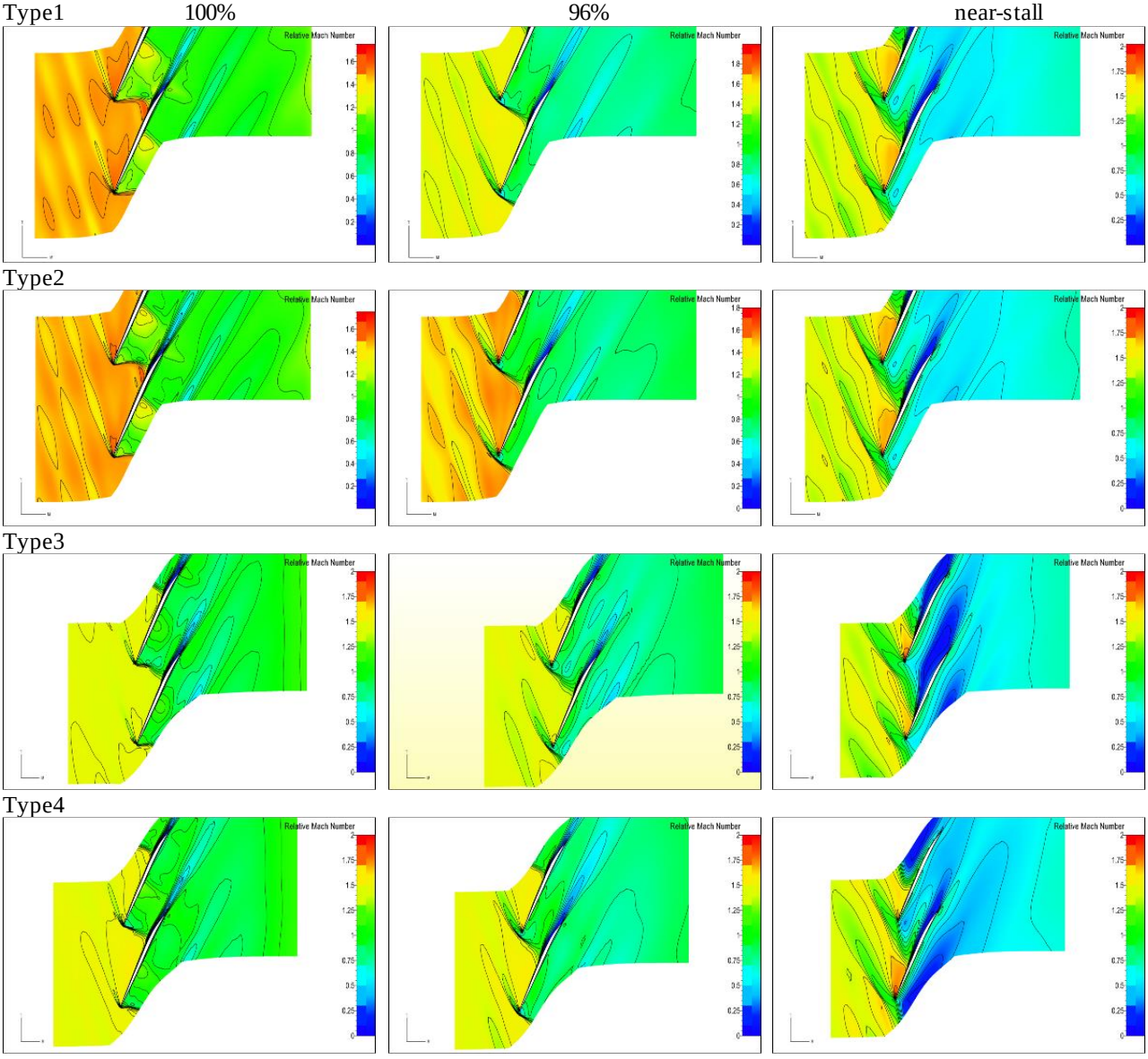

Figure 8 Comparison of relative Mach number at 95% span

with the decrease of mass flow, the low Mach number area is expanded from the trailing edge to the blade suction surface. And this expanding process would be prevented by the shock wave before the leading edge. The phenomenon can be observed obviously in type 3 and type 4 at near-stall point, which that the low Mach number areas are different in two passages. Meanwhile, these areas were prevented by the shock wave, too. The shock wave can reach a deeper position in passages for the alternate swept rotor types, which leads to that low Mach number area was kept in rearward position in one passage, while the low Mach number area deteriorated in adjacent passage. As we all known, the low Mach number areas can be considered as rotating stall areas. For the rotors swept holistically, the rotating stall would be expanded to whole flow field. Concurrently, the rotating stall can't be expanded to whole field because the adjacent passage can stay in stable condition with the rotor swept alternately. It is also lead to a decrease in adiabatic efficiency and total pressure ratio which can be observed in Figure 6.

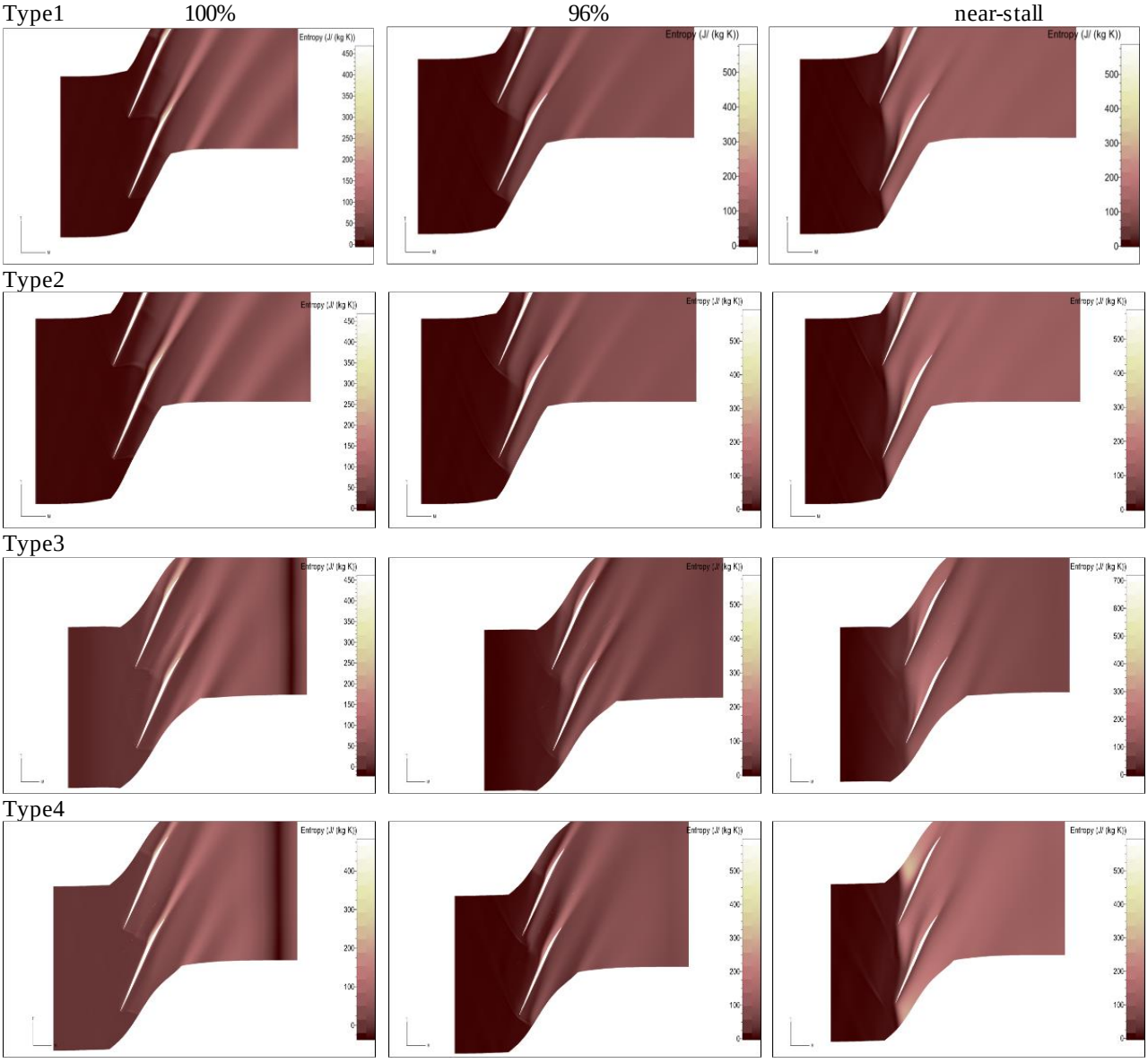

Figure 9 Comparison of Entropy at 95% span

Figure 9 shows the Entropy at 95% span. It is also the comparison for 4 rotor types at three different points. According to the research of Vo et al.[6], the phenomena that the interface between the tip clearance and oncoming flows becomes parallel to the leading-edge plane leads to the onset of short length-scale (spike) rotating stall disturbances. This was demonstrated in Figure 9. The processes of interface moving forward are different in adjacent passage for type 3 and type 4. It means that interface becomes parallel to the leading edge in one passage, while the interface in adjacent passage is still on the processing of moving forward. The interface moving was influenced by tip clearance which can be anlyzed in Figure 10.

Figure 10 shows the tip clearance streamlines for these conditions. From the type 1 and type 2, the interface moving can be observed. The tip clearance was accumulated in the leading edge of blade. And the rearward position of the

passage was showed as blank, which means that it is rotating stall, as showed in Figure 8 and Figure 9. For the types with rotor swept alternately, rotating stall was developed in a serious condition, while flow was still kept stable in suction surface of adjacent blade.

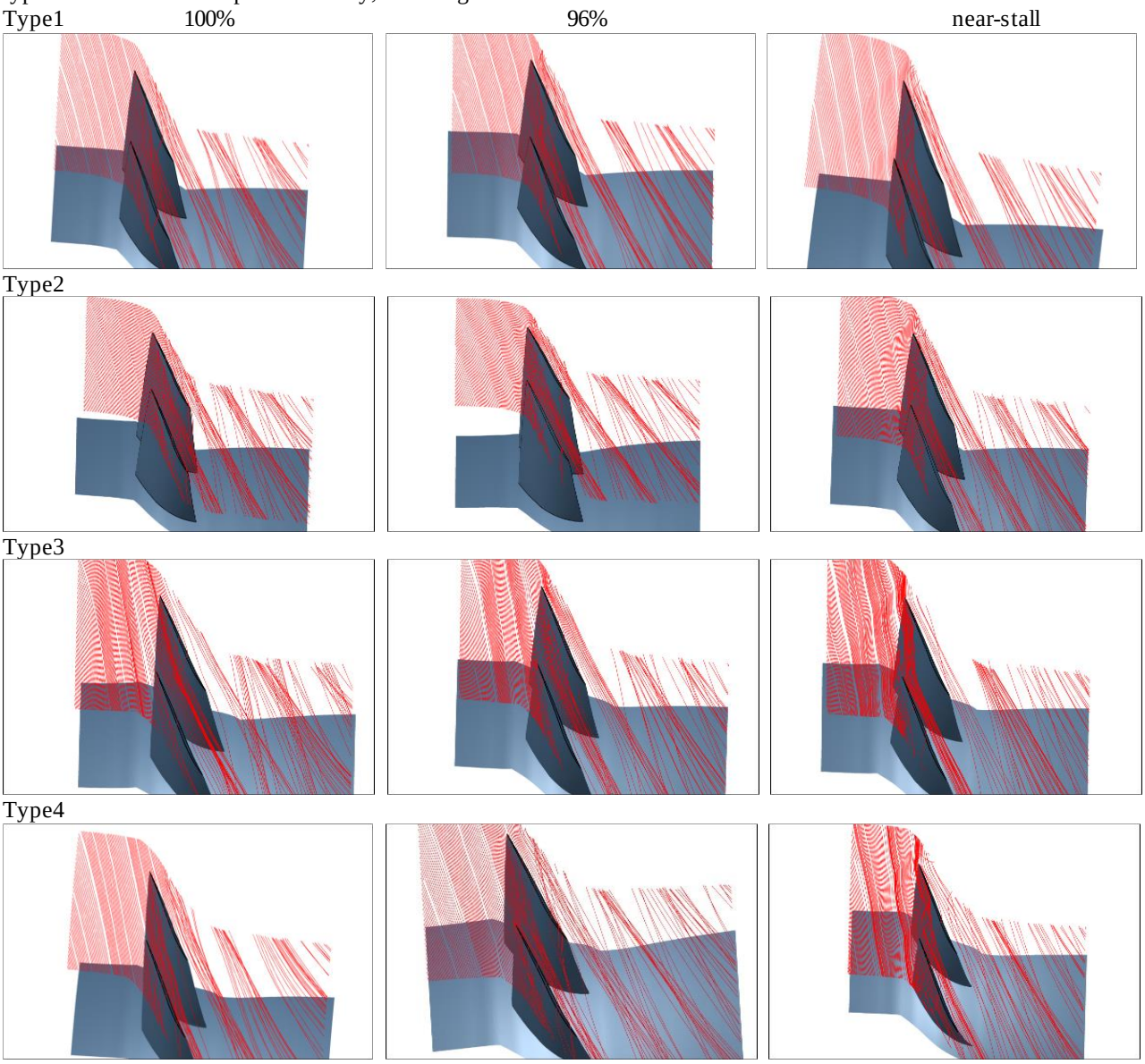

Figure 10 Comparison of streamlines in tip region

The distance between leading edge of blades was enhanced for the rotor swept alternately. The tip leakage mostly inflows to the passages, which has a smaller effect on the tip clearance flow of adjacent blades. The tip clearance flow can interact on each other blades from Type 1 and Type 2. The phenomena lead to the stall margin improvement, which the flow accumulated in the leading edge had smaller influence on adjacent tip clearance. As showed in Figure 8, the rotating stall can't be expanded to whole flow field, because the adjacent passage can stay in stable condition.

5 Conclusions

In this paper, the effects of rotor swept alternately or holistically on the stall margin are investigated. A novel rotor type is presented, which integrates an improved stall margin. Three new types are modelled based on the NASA Rotor 37. The results are summarized as followed.

The rotors with swept alternately achieve a significant improvement in stall margin, while the rotor with swept holistically has no influence on overall performance and details of flow field. The stall margin of new rotor types can reach up to 18.16%, while that of the original rotor is only 9.71%. The efficiency of rotors with swept alternately are slightly underestimated in the peak zone (by about 0.93%

and 1.16%), while the total pressure ratio is slightly underestimated by about 1.53% and 2.82%.

The flow fields are different which are showed between the rotors with swept alternately and other rotor types. For the types with rotor swept alternately, flow stability is showed different in different passage. Rotating stall was developed in a serious condition, while flow was still kept stable in suction surface of adjacent blade. It means the rotor can be operated at a lower mass flow rate. As expected, a decrease of adiabatic efficiency was obtained by these rotors swept.

The distance between leading edge of blades was enhanced for the rotor swept alternately. The rotor swept alternately reduces the interaction of tip clearance flow between adjacent blades.

Acknowledged

The first author greatly appreciates the support from China Scholarship Council. This work is also supported by Natural Science Foundation of China (No. 51576124, No. 51506126). The support from the United Innovation Center (UIC) of Aerothermal Technologies for Turbomachinery is also acknowledged.

References

1. Kai, Z.（2008）, The investigation of the tip clearance flow of axial flow compressor with adjustable tip additional blades., Harbin Institute of Technology: Harbin.
2. Paduano, J., Epstein, A. H., Valavani, L., Longley, J. P., Greitzer, E. M., & Guenette, G. R. (1991, June). Active control of rotating stall in a low speed axial compressor. In ASME 1991 International Gas Turbine and Aeroengine Congress and Exposition (pp. V001T01A036-V001T01A036). American Society of Mechanical Engineers.
3. Day, I. J. (1991, June). Stall inception in axial flow compressors. In ASME 1991 International Gas Turbine and Aeroengine Congress and Exposition (pp. V001T01A034-V001T01A034). American Society of Mechanical Engineers.
4. Houghton, T., & Day, I. (2011). Enhancing the stability of subsonic compressors using casing grooves. Journal of Turbomachinery, 133(2), 021007.
5. RUKAVINA, J., OKIISHI, T., & WENNERSTROM, A. (1990). Stall margin improvement in axial-flow compressors by circumferential variation of stationary blade setting angles. In 26th Joint Propulsion Conference (p. 1912).
6. Vo, H. D., Tan, C. S., & Greitzer, E. M. (2008). Criteria for spike initiated rotating stall. Journal of turbomachinery, 130(1), 011023.
7. Pullan, G., Young, A. M., Day, I. J., Greitzer, E. M., & Spakovszky, Z. S. (2015). Origins and structure of spike-type rotating stall. Journal of Turbomachinery, 137(5), 051007.
8. Tan, C. S., Day, I., Morris, S., & Wadia, A. (2010). Spike-type compressor stall inception, detection, and control. Annual review of fluid mechanics, 42, 275-300.
9. Ahn, C. S., & Kim, K. Y. (2002). Aerodynamic design optimization of an axial compressor rotor. ASME Paper GT-2002-30445.
10. Denton, J. D., & Xu, L. (1998). The exploitation of three-dimensional flow in turbomachinery design. Proceedings of the Institution of Mechanical Engineers, Part C: Journal of Mechanical Engineering Science, 213(2), 125-137.
11. Yamaguchi, N. (1991). Secondary-loss reduction by forward-skewing of axial compressor rotor blading. 91-YOKOHAMA, 8.
12. Hah, C., Puterbaugh, S. L., & Wadia, A. R. (1998, June). Control of shock structure and secondary flow field inside transonic compressor rotors through aerodynamic sweep. In ASME 1998 International Gas Turbine and Aeroengine Congress and Exhibition (pp. V001T01A132-V001T01A132). American Society of Mechanical Engineers.
13. Wadia, A. R., Szucs, P. N., & Crall, D. W. (1997, June). Inner workings of aerodynamic sweep. In ASME 1997 International Gas Turbine and Aeroengine Congress and Exhibition (pp. V001T03A062-V001T03A062). American Society of Mechanical Engineers.
14. Denton, J. D., & Xu, L. (2002, January). The effects of lean and sweep on transonic fan performance. In ASME Turbo Expo 2002: Power for Land, Sea, and Air (pp. 23-32). American Society of Mechanical Engineers.
15. He, C., Ma, Y., Liu, X., Sun, D., & Sun, X. (2018). Aerodynamic instabilities of swept airfoil design in transonic axial-flow compressors. AIAA Journal, 1878-1893.
16. Moore, R. D., & Reid, L. (1980). Performance of single-stage axial-flow transonic compressor with rotor and stator aspect ratios of 1.19 and 1.26 respectively, and with design pressure ratio of 2.05.
17. Benini, E., & Biollo, R. (2006, January). On the aerodynamics of swept and leaned transonic compressor rotors. In ASME Turbo Expo 2006: Power for Land, Sea, and Air (pp. 283-291). American Society of Mechanical Engineers.
18. He, C., Sun, D., & Sun, X. (2018). Stall Inception Analysis of Transonic Compressors With Chordwise and Axial Sweep. Journal of Turbomachinery, 140(4), 041009.
19. Dunham, J. (1998). CFD validation for propulsion system components (la validation CFD des organes des propulseurs) (No. AGARD-AR-355). ADVISORY GROUP FOR AEROSPACE RESEARCH AND DEVELOPMENT NEUILLY-SUR-SEINE (FRANCE).
20. Allmaras, S. R., & Johnson, F. T. (2012, July). Modifications and clarifications for the implementation of the Spalart-Allmaras turbulence model. In Seventh international conference on computational fluid dynamics (ICCFD7) (pp. 1-11).